16. Z. Yao, C. L. Kane, C. Dekker, *Phys. Rev. Lett.* **84**, 2941 (2000).
17. At 30 K, the mobility of the potassium atoms is substantially reduced as compared to that at 90 K, where the condensed phase of potassium atoms is found (*18*). It is thus reasonable to assume that the potassium atoms mainly adsorb onto and interact with the surface of the graphene layer in the low-temperature deposition we used (around 30 K).
18. K. M. Hock, R. E. Palmer, *Surf. Sci.* **284**, 349 (1993).
19. Y. Zhang, J. P. Small, W. V. Pontius, P. Kim, *Appl. Phys. Lett.* **86**, 073104 (2005).
20. K. S. Novoselov, F. Schedin, D. Jiang, A. A. Firsov, A. K. Geim, *Phys. Rev. B* **72**, 201401 (2005).
21. I. Forbeaux, J.-M. Themlin, J.-M. Debever, *Phys. Rev. B* **58**, 16396 (1998).
22. J. N. Crain, K. N. Altmann, C. Bromberger, F. J. Himpsel, *Phys. Rev. B* **66**, 205302 (2002).
23. Eli Rotenberg *et al.*, *Phys. Rev. Lett.* **91**, 246404 (2003).
24. J. C. Slonczewski, P. R. Weiss, *Phys. Rev.* **109**, 272 (1958).
25. J. W. McClure, *Phys. Rev.* **108**, 612 (1957).
26. S. V. Morozov *et al.*, *Phys. Rev. B* **72**, 201401 (2005).
27. This work and the Advanced Light Source were supported by the U.S. Department of Energy, Office of Basic Sciences. K.H. and T.O. were supported by the Max Planck Society and the European Science Foundation under the EUROCORES SONS program.

Supporting Online Material
www.sciencemag.org/cgi/content/full/313/5789/952/DC1
Materials and Methods
Figs. S1 to S3
References

31 May 2006; accepted 12 July 2006
10.1126/science.1130681

Two-Dimensional Nematic Colloidal Crystals Self-Assembled by Topological Defects

Igor Muševič,[1,2]* Miha Škarabot,[1] Uroš Tkalec,[1] Miha Ravnik,[2] Slobodan Žumer[2,1]

The ability to generate regular spatial arrangements of particles is an important technological and fundamental aspect of colloidal science. We showed that colloidal particles confined to a few-micrometer-thick layer of a nematic liquid crystal form two-dimensional crystal structures that are bound by topological defects. Two basic crystalline structures were observed, depending on the ordering of the liquid crystal around the particle. Colloids inducing quadrupolar order crystallize into weakly bound two-dimensional ordered structure, where the particle interaction is mediated by the sharing of localized topological defects. Colloids inducing dipolar order are strongly bound into antiferroelectric-like two-dimensional crystallites of dipolar colloidal chains. Self-assembly by topological defects could be applied to other systems with similar symmetry.

Dispersions of colloids or liquid droplets in a nematic liquid crystal show a diversity of self-assembled structures, such as linear chains (*1*, *2*), anisotropic clusters (*3*), two-dimensional (2D) hexagonal lattices at interfaces (*4*, *5*), arrays of defects (*6*), particle-stabilized gels (*7*), and cellular soft-solid structures (*8*). The ability of liquid crystals to spontaneously arrange foreign particles into regular geometric patterns is therefore highly interesting for developing new approaches to building artificial colloidal structures, such as 3D photonic band-gap devices (*9*). Current approaches to fabrication rely on the controlled sedimentation of colloids from solutions (*10*), growth on patterned and prefabricated templates on surfaces (*11*), external-field–assisted manipulation (*12*), and precision lithography combined with mechanical micromanipulation (*13*).

In isotropic solvents, the spatial aggregation of colloids is controlled by a fine balance between the attractive dispersion forces and the Coulomb, steric, and other repulsive forces. The nature of colloidal interactions in nematic liquid crystals is quite different. Nematic liquid crystals are orientationally ordered complex fluids, in which rodlike molecules are spontaneously and collectively aligned into a certain direction, called the director. Because of their anisotropy, the orientation of nematic liquid crystals can be manipulated by external electric or magnetic fields, or even by anisotropic surfaces, which is an important issue in liquid crystal display technology. When foreign particles are introduced into the nematic liquid crystal, the orientation of nematic molecules is locally disturbed because of their interaction with the surfaces of the inclusions. The disturbance spreads on a long (micrometer) scale and can be considered as an elastic deformation of the nematic liquid crystal. Because the elastic energy of deformation depends on the separation between inclusions, structural forces between inclusions are generated. The structural forces in liquid crystals are long-range (on the order of micrometers) and spatially highly anisotropic, thus reflecting the nature of the order in liquid crystals (*14*–*17*).

In our experiments, a dispersion of micrometer-sized silica spheres in the nematic liquid crystal pentylcyanobiphenyl (5CB) was introduced into a rubbed thin glass cell with thickness varying along the direction of rubbing from

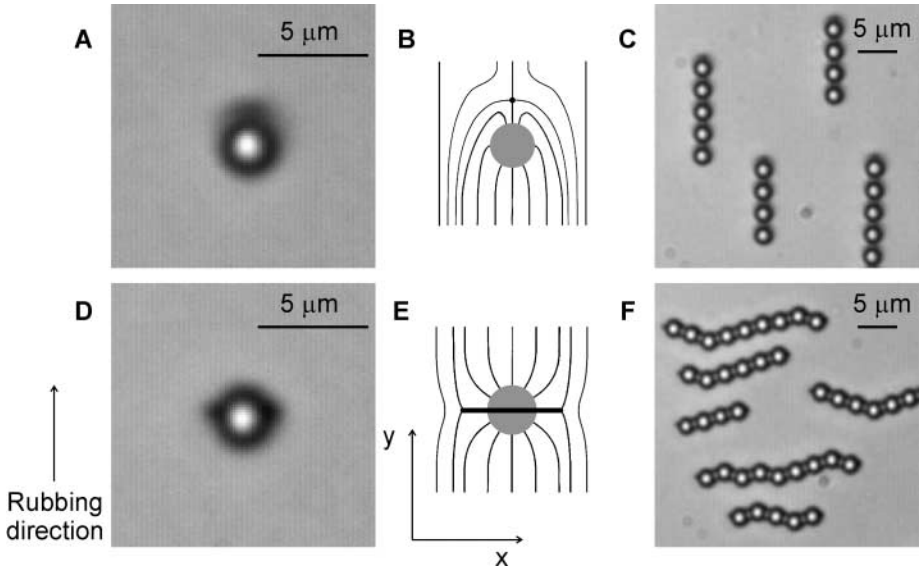

Fig. 1. Dipolar and quadrupolar colloids in a thin layer of a nematic liquid crystal. (**A**) Micrograph of a $d = 2.32$ μm silica sphere in an $h = 5$ μm layer of 5CB with a hyperbolic hedgehog defect (black spot on top). (**B**) The nematic order around the colloid has the symmetry of an electric dipole. (**C**) Dipoles spontaneously form dipolar (ferroelectric) chains along the rubbing direction. (**D**) The same type of colloid in a thin ($h = 2.5$ μm) 5CB layer. The two black spots on the right and left side of the colloid represent the Saturn ring. (**E**) The nematic order has in this case the symmetry of an electric quadrupole. (**F**) Quadrupoles spontaneously form kinked chains perpendicular to the direction of rubbing.

[1]J. Stefan Institute, Jamova 39, 1000 Ljubljana, Slovenia. [2]Faculty of Mathematics and Physics, University of Ljubljana, Jadranska 19, 1000 Ljubljana, Slovenia.

*To whom correspondence should be addressed. E-mail: igor.musevic@ijs.si

one to several colloidal diameters [supporting online material (SOM), section 1]. The colloidal surfaces were treated chemically to induce perpendicular surface orientation of the 5CB, whereas the surfaces of the confining cell were treated to induce parallel orientation. The resulting elastic distortion of the 5CB around the colloids generated repulsive forces between the colloids and the walls of the cell, thus elastically stabilizing the colloids in the middle of the nematic layer. In thinner parts of the cell, the colloids were surrounded by a distorted nematic liquid crystal that had a director field with a symmetry reminiscent of that of an electric quadrupole (*18*–*21*). In thicker parts, the nematic liquid crystal around the colloids had a symmetry like that of an electric dipole (*1*, *2*, *18*, *19*).

Figure 1A shows a micrograph of a silica sphere with diameter $d = 2.32 \pm 0.02$ μm in a nematic layer with a thickness (h) of 5 μm. The structure of the director field around the colloid is shown in Fig. 1B. It is distorted dipolarly, with a hyperbolic hedgehog defect (*18*, *19*) that appears as a dark spot on the top of the colloid in Fig. 1A. The colloid and the hedgehog are oriented along the rubbing direction (the y axis in Fig. 1), thus forming an analog of an electric dipole (*22*, *23*). Dipoles spontaneously assemble into dipolar (ferroelectric-like) chains oriented along the rubbing direction (Fig. 1C). For thickness smaller than the critical one $h_c = 3.5 \pm 0.1$ μm, the dipolar field around the colloid is strongly influenced by the confining surfaces. The symmetry of the director field around the colloid is now quadrupolar (Fig. 1E), with a closed disclination line (Saturn ring) surrounding the colloid (*24*). The two black spots on the right and left side of the colloid in Fig. 1D represent the top view of the Saturn ring, encircling the colloid. Quadrupolar colloids spontaneously self-assemble into kinked chains oriented perpendicular to the rubbing direction (Fig. 1F).

In the experiments, laser tweezers were used to position colloids (*25*) and assist their assembly into stable 2D structures. The temporal position of the colloids was video-monitored by means of an optical microscope and image capture. Analysis of the colloidal trajectories (*25*) allowed us to determine the separation dependence of the structural forces between colloids and the binding energy of colloids in colloidal assemblies.

Figure 2 shows time sequences of the self-assembly of quadrupolar colloids in a thin cell. A single pair of quadrupolar colloids is attracted at an angle of ~73°, measured from the rubbing direction (Fig. 2A), which promotes the growth of kinked quadrupolar chains in a direction perpendicular to rubbing (Fig. 2, B and C). Comparison of Fig. 2, B and C, shows that an additional colloid can either be added to a position that creates an additional kink or promote the growth of straight chains that are tilted with respect to the rubbing direction. Figure 2D shows that the additional colloid is also attracted laterally to an already-formed chain and promotes the growth of truly 2D quadrupolar colloidal crystals. The colloids are in all cases attracted to a specific position, already at a separation of several micrometers, which demonstrates the long-range and anisotropic nature of structural nematic forces. The measured binding energy of an additional quadrupole, attracted along the kinked quadrupolar chain, is ~3.4×10^{-18} J (~800 k_BT). The measured lateral attraction of an isolated quadrupole toward the side of a quadrupolar chain is much weaker (~120 k_BT) than the binding energy of a colloid in a quadrupolar chain. A stack of quadrupolar chains can rearrange in an almost hexagonal structure with a more symmetric distribution of Saturn ring defects.

An example of directed 2D assembly of quadrupolar colloidal crystal is shown in Fig. 2E. A single colloid was positioned with laser tweezers close to a crystallite and released from the optical trap. The sequence of images demonstrates the attraction of an isolated colloid into the unoccupied corner of a small crystallite. The structural force between an isolated colloid and an already formed quadrupolar 2D nematic crystallite was attractive when the colloid approached the chain at its ends. When the colloid approached the chain or an already-formed crystallite in a lateral direction, the force was at first repulsive, but when the colloid was forced closer to the chain, it formed nematic bonds with the chain. The measured elastic attractive potential for the sequence in Fig. 2E is presented in Fig. 2F, demonstrating strong attraction over large separations of more than 5 μm. As a result, stable 2D crystals with oblique 2D lattices were assembled (Fig. 2G), which were stable over a time period of several days. The shape of the unit cell was that of a general parallelogram with $a = 2.69 \pm 0.04$ μm, $b = 3.01 \pm 0.05$ μm, and $\gamma = 56° \pm 1°$. We also observed that such 2D quadrupolar nematic colloidal crystals were quite susceptible to external perturbations, such

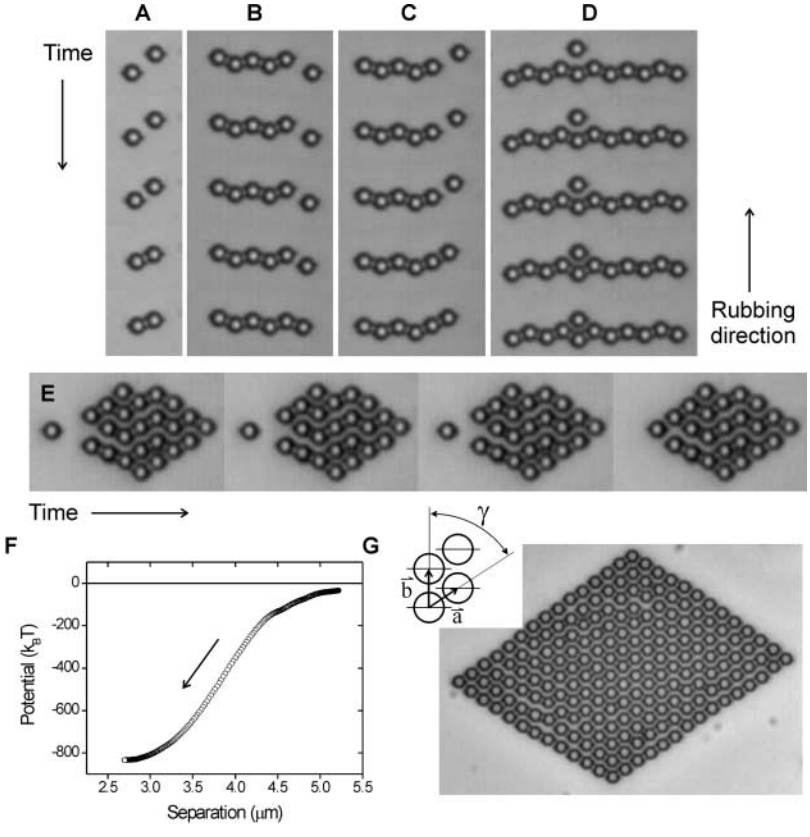

Fig. 2. Growth of 2D quadrupolar nematic colloidal crystals. (**A**) Time sequence showing the spontaneous assembly of a quadrupolar pair of colloids. An additional colloid is attracted to the chain: (**B**) into a position that creates a kink, (**C**) in a straight and tilted line, or (**D**) laterally. The time between individual frames in (A) to (C) was 0.8 s and 2.2 s in (D). The cell thickness was $h = 2.7$ μm. (**E**) Directed assembly of quadrupolar colloids in a 2D crystal. The colloid was positioned close to the corner of an already formed crystallite and released. Directed attraction into a unoccupied corner due to the structural force is clearly shown. The time difference between individual frames was 5 s. (**F**) Measured elastic energy of the colloid as a function of its separation from the unoccupied corner position (*25*). The arrow indicates the direction of movement of the colloid. (**G**) Large quadrupolar crystal formed by directed assembly by means of laser tweezers.

as flow of the nematic liquid crystal due to external pressure, change of temperature, etc. This indicates the existence of a huge variety of metastable structures within an ensemble of ordered quadrupolar nematic colloids in thin nematic layers.

At large cell thickness, colloids are dipolar and tend to spontaneously form linear chains along the rubbing direction (*1*, *2*). We have measured the binding energy of a single dipolar colloid in a dipolar chain, which is ~4500 k_BT and is much stronger than the binding energy of a single quadrupole in a quadrupolar chain. We visualize these dipolar chains as 1D "ferroelectric" objects, polarized along the direction of their dipoles.

The structural force between an isolated dipolar colloid and the ferroelectric colloidal chain depends on the orientation of the dipolar colloid, as shown in two time sequences in Fig. 3, A and B. For the parallel orientation of the dipoles (Fig. 3A), the colloid is repelled from the ferroelectric chain, whereas for the antiparallel orientation of the dipoles (Fig. 3B), the colloid is strongly attracted toward the chain. The measured elastic dipolar potentials are shown in Fig. 3C for parallel and antiparallel orientation. The measured elastic potential of lateral attraction is extremely strong at micrometer separation (~3000 k_BT) and is much stronger than the lateral attraction in quadrupolar chains. At close proximity, the separation between the colloids is stabilized by the hyperbolic hedgehog defect, generating short-range repulsive structural force (*18*, *19*). The combination of a long-range attraction and short-range elastic repulsion thus allows us to grow stable 2D dipolar nematic crystals, as shown in Fig. 3D. The crystal is easily formed by pairs of antiparallel ferroelectric colloidal chains that form a parallelogram unit cell with lattice constants $a = 2.95 \pm 0.03$ μm, $b = 2.84 \pm 0.02$ μm, and $\gamma = 61° \pm 1°$. This corresponds to a 520-nm surface-surface separation between colloids along the chains and a 640-nm separation between the nearest colloids in sequent ferroelectric chains. The crystal structure is extremely robust against external perturbations and remains stable for several weeks. As an illustration of its robustness, the crystal can be grabbed by laser tweezers and moved to a new position as a single unit (fig. S1).

In order to identify the binding mechanism and to prove that it is indeed liquid crystal that stabilizes our colloidal crystals, we examined the system with numerical modeling. When dealing with small colloidal particles and defects in liquid crystals, a Landau–de Gennes description based on the nematic order parameter tensor $Q_{ij} = S/2(3n_in_j - \delta_{ij})$ is most appropriate, as it takes into account not only Frank elasticity due to deformation (*18*, *19*) but also local variations of the degree of order. The order parameter tensor is a 3 × 3 symmetric traceless matrix, whose invariants are used to phenomenologically construct the free energy F of the nematic, constrained by colloidal particles and surfaces of the cell (*26*)

$$F = +\frac{1}{2}L\int_{LC}\left(\frac{\partial Q_{ij}}{\partial x_k}\right)\left(\frac{\partial Q_{ij}}{\partial x_k}\right)dV + \int_{LC}\left(\frac{1}{2}AQ_{ij}Q_{ji} + \frac{1}{3}BQ_{ij}Q_{jk}Q_{ki} + \frac{1}{4}C(Q_{ij}Q_{ji})^2\right)dV + \frac{1}{2}W\int_{Surf.Col.}(Q_{ij} - Q^0_{ij})(Q_{ji} - Q^0_{ji})dS. \quad (1)$$

The first term in Eq. 1 represents the increase of the free energy due to spatial variations of the nematic order, whereas the second term represents the contribution to the free energy due to the nematic order. The interaction of the nematic liquid crystal with the surfaces of the colloids is represented by the third term. We chose a single elastic constant approximation (L); A, B, and C are conventional nematic material constants; W is the strength of surface anchoring; and Q^0_{ij} is the order parameter preferred by the surface (SOM, section 3). We set the orientation of the nematic molecules parallel to the surfaces of the cell with the bulk value of the order parameter. The free energy therefore covers all three fundamental liquid crystal phenomena relevant to our experiments: elasticity, the possible formation of defects, and the finite interaction of a liquid crystal with the surfaces of the colloids.

The minimum of the free energy is found by solving a system of coupled nonlinear partial differential equations with relevant boundary conditions (SOM, section 4). We did this numerically by an explicit Euler finite difference relaxation algorithm on a cubic mesh (*27*). Colloids with both quadrupolar and dipolar symmetry appear as possible solutions. Results for a particular choice of parameter values (*28*) are presented in Fig. 4.

In the case of 2D nematic quadrupoles, numerical calculations reproduce the experiments very well. Figure 4, A and B, show one of the stable solutions for the 2D nematic quadrupolar colloidal crystals, where the director field with local quadrupolar symmetry is periodic in two dimensions. In this case, the orientational defects (Saturn rings) are localized around nearly hexagonally packed colloids. The binding force between colloids comes from sharing of the elastically distorted region around individual colloids. At equilibrium, the lattice constants of an oblique 2D lattice are $a = 1.15d$ and $b = 1.32d$,

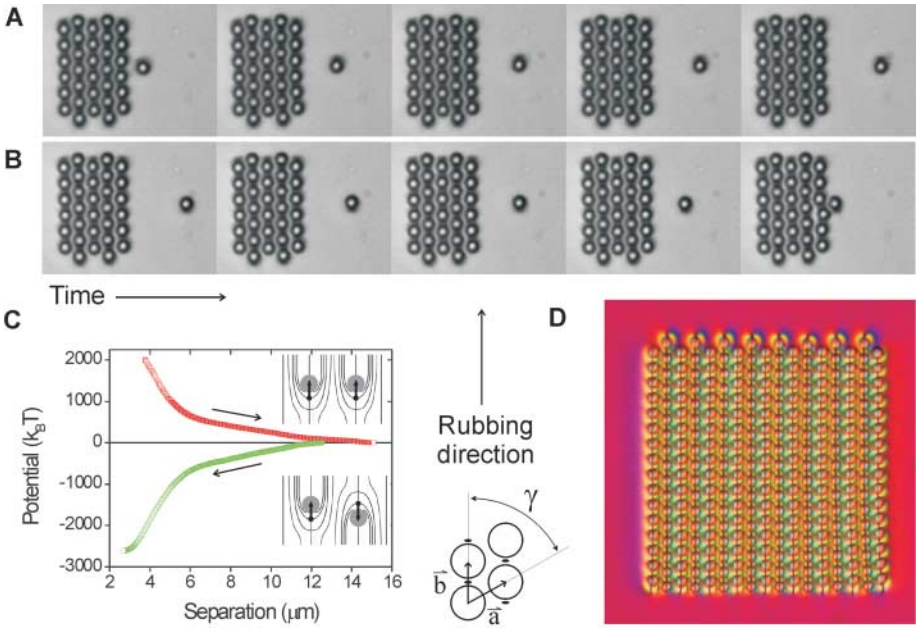

Fig. 3. Assembly of dipolar colloids into 2D nematic colloidal crystals. (**A**) A dipolar nematic colloid is repelled from the neighboring ferroelectric chain if its dipole is parallel to the dipoles in the chain. The time difference between images was 4 s. (**B**) The colloid is attracted to the chain if its dipole is antiparallel to the dipoles in the chain. The time difference between images was 4 s. (**C**) Measured attractive and repulsive elastic potential for two different orientations of the colloidal dipole. Arrows indicate the direction of movement of the colloid (*25*). Like dipoles are repelled from and unlike dipoles are attracted to the chain. (**D**) A 2D dipolar colloidal crystal formed by pairs of antiparallel dipolar chains. Different colors represent different orientations of the nematic molecules.

with $\gamma = 55°$, which is in perfect agreement with the experimental values $a = 1.16d$, $b = 1.3d$, $\gamma = 56°$. We have also calculated the free energy of such a 2D quadrupolar crystal after "stretching" it in x and y directions, which is shown in Fig. 4C. The minimum of the free energy (green area) indeed proves that colloids are bound collectively in two dimensions by liquid crystal Frank elasticity. In addition we have estimated the effective binding force $\mathcal{F} = -\partial F/\partial x$ per colloid bond. At a colloid separation increase of $0.1d$, one finds $\mathcal{F} = -13$ pN, which is roughly comparable to the experimental value of –3 pN. The material constants were not optimized to fit the experiment.

A stable 2D colloidal structure with local dipolar symmetry of the director field is presented in Fig. 4, D and E. Because of the strong confinement set by the nematic orientation at the surface of the thin cell (*28*), the hyperbolic hedgehog defect has "opened" and appears in a form of a small defect ring with the same topological properties. This reduces the separation along the dipolar chains and enhances the anisotropy of the lattice. The lattice constants of the oblique 2D lattice are $a = 1.26d$ and $b = 1.01d$, with $\gamma = 66°$, which is in agreement with the experimental values $a = 1.27d$, $b = 1.23d$, $\gamma = 61°$. The free energy landscape F for 2D dipolar colloids is presented in Fig. 4F. Compared to the quadrupolar case (Fig. 4C), the potential well is much steeper, indicating much stronger and anisotropic binding. In particular, bonds between dipolar colloids are extremely strong along the direction of dipolar chains and relatively weaker between the chains. As a result of strong confinement, imposed in our calculations (and consequent opening of the hyperbolic hedgehog defect), the dipoles are so strongly attracted along the chain that their surfaces actually touch. This is evidenced by the green area in the energy landscape in Fig. 4F, which indicates that at equilibrium, the colloids are touching each other along the chain. Nevertheless, the numerical analysis clearly proves the existence of collectively bound dipolar colloids in two dimensions.

The main result of our work is that stable and long-range–ordered nematic colloidal crystals exist in thin nematic layers. Unlike forces that are responsible for the long-range order of colloids in isotropic host liquids, the forces that bind nematic colloids together are of structural origin and therefore much richer in the sense of their anisotropy. We have found two different types of 2D nematic colloidal crystals in our experiments: those with quadrupolar and dipolar symmetry. In both cases, the binding mechanism is the same and represents a fine balance between two basic mechanisms: (i) the colloids minimize the total free energy of elastically distorted nematic crystals by approaching each other and thus sharing topological defects (regions of distortion) with each other; and (ii) when colloids are in close proximity, repulsive structural forces are generated because of strong spatial variation of the nematic order. A delicate balance between these two effects governs the positional and orientational ordering of nematic colloidal crystals.

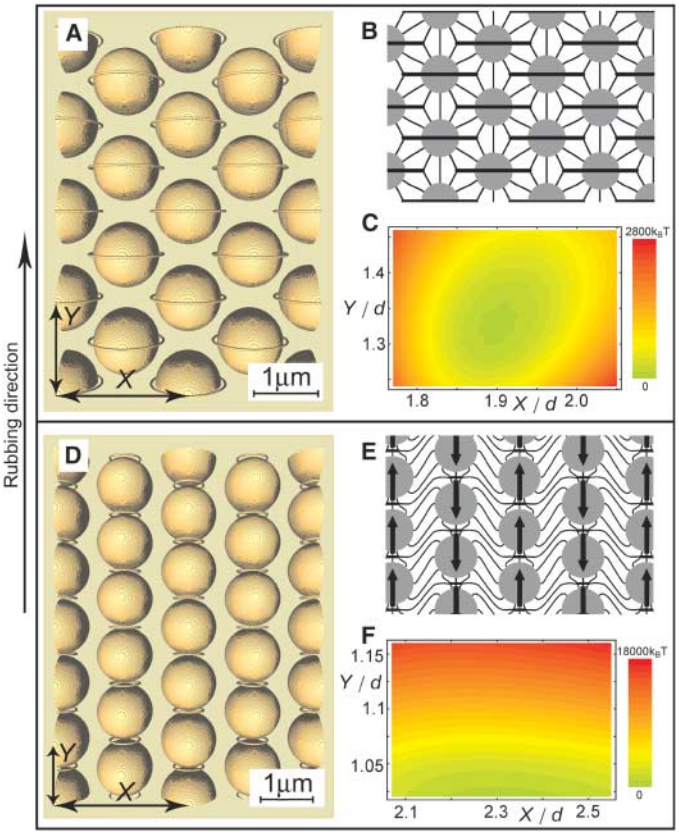

Fig. 4. Stable quadrupolar and dipolar nematic colloidal crystals in two dimensions. (**A**) Crystal with quadrupolar symmetry. The Saturn defects are localized and surround the colloids. The image represents isosurfaces, where the magnitude of the order parameter is $S = 0.45$. (**B**) Schematic view of the quadrupolar director field, with the heavy line representing the Saturn defect. (**C**) Free energy landscape F, calculated for a unit cell with a total of two quadrupolar colloids bound by Saturn defects. (**D**) Stable 2D crystal with dipolar symmetry. The hyperbolic hedgehog defects have opened because of the strong confinement. Again, a surface with $S = 0.45$ is shown. (**E**) Schematic view of a 2D stable crystal of dipolar nematic colloids. The arrows indicate the direction of the topological dipole; note the antiferroelectric arrangement of dipoles. Thin lines represent the local direction of nematic molecules. (**F**) Calculated F for a unit cell with a total of two dipolar colloids.

References

1. P. Poulin, H. Stark, T. C. Lubensky, D. A. Weitz, *Science* **275**, 1770 (1997).
2. J. C. Loudet, P. Barois, P. Poulin, *Nature* **407**, 611 (2000).
3. P. Poulin, D. A. Weitz, *Phys. Rev. E* **57**, 626 (1998).
4. V. G. Nazarenko, A. B. Nych, B. I. Lev, *Phys. Rev. Lett.* **87**, 075504 (2001).
5. I. I. Smalyukh *et al.*, *Phys. Rev. Lett.* **93**, 117801 (2004).
6. M. Yada, J. Yamamoto, H. Yokoyama, *Langmuir* **18**, 7436 (2002).
7. M. Zapotocky, L. Ramos, P. Poulin, T. C. Lubensky, D. A. Weitz, *Science* **283**, 209 (1999).
8. S. P. Meeker, W. C. K. Poon, J. Crain, E. M. Terentjev, *Phys. Rev. E* **61**, R6083 (2000).
9. S. Noda, T. Baba, Eds., *Roadmap on Photonic Crystals* (Kluwer Academic, Dordrecht, Netherlands, 2003).
10. V. W. A. de Villeneuve *et al.*, *Science* **309**, 1231 (2005).
11. A. van Blaaderen, R. Ruel, P. Wiltzius, *Nature* **385**, 321 (1997).
12. P. Y. Chiou, A. T. Ohta, M. C. Wu, *Nature* **436**, 370 (2005).
13. K. Aoki *et al.*, *Nat. Mater.* **2**, 117 (2003).
14. J. C. Loudet, P. Poulin, *Phys. Rev. Lett.* **87**, 165503 (2001).
15. M. Yada, J. Yamamoto, H. Yokoyama, *Phys. Rev. Lett.* **92**, 185501 (2004).
16. I. I. Smalyukh, O. D. Lavrentovich, A. N. Kuzmin, A. V. Kachynski, P. N. Prasad, *Phys. Rev. Lett.* **95**, 157801 (2005).
17. T. Araki, H. Tanaka, *J. Phys. Condens. Matter* **18**, L193 (2006).
18. T. C. Lubensky, D. Pettey, N. Currier, H. Stark, *Phys. Rev. E* **57**, 610 (1998).
19. H. Stark, *Phys. Rep.* **351**, 387 (2001).
20. N. Yuedong Gu Abbott, *Phys. Rev. Lett.* **85**, 4719 (2000).
21. H. Stark, *Phys. Rev. E* **66**, 032701 (2002).
22. O. D. Lavrentovich, *Liquid Crystals* **24**, 117 (1998).
23. Similar to charges in electrostatics, topological defects in nematics are sources (and sinks) of the director field. Defects, such as hedgehogs, are characterized by integer topological charge, specifying the number of times that the unit sphere is wrapped by all the directors around the defect core. A point defect (hedgehog) with charge 1 can open into a line defect (Saturn ring) with the same charge.
24. A similar transformation was predicted for dipolar colloids in an external magnetic field (*19*).
25. M. Škarabot *et al.*, *Phys. Rev. E* **73**, 021705 (2006).
26. P. G. de Gennes, J. Prost, *The Physics of Liquid Crystals* (Oxford Science Publications, Oxford, ed. 2, 1993).
27. W. H. Press, B. P. Flannery, S. A. Teukolsky, W. T. Vetterling, *Numerical Recipes* (Cambridge Univ. Press, Cambridge, 1986).
28. In both quadrupolar and dipolar calculations, the following numerical values for parameters were used: $A = -0.172 \times 10^6$ J/m^3, $B = -2.12 \times 10^6$ J/m^3, $C = 1.73 \times 10^6$ J/m^3,

$L = 4.0 \times 10^{-11}$ N, $W = 1.0 \times 10^{-2}$ J/m^2. The diameter of the colloids was 1.0 μm and the cell thickness was 2.0 μm. For this particular choice of parameter values, both configurations are stable. The quadrupole is metastable with respect to the dipole, and therefore by only changing the initial conditions for the relaxation algorithm, either dipolar or quadrupolar defect structures were generated. Periodic boundary conditions in x and y directions were used.

Supporting Online Material
www.sciencemag.org/cgi/content/full/313/5789/954/DC1
Materials and Methods
Fig. S1
References

8 May 2006; accepted 6 July 2006
10.1126/science.1129660

Switchable Surfactants

**Yingxin Liu,[1] Philip G. Jessop,[1]* Michael Cunningham,[1]
Charles A. Eckert,[2] Charles L. Liotta[2]**

Many industrial applications that rely on emulsions would benefit from an efficient, rapid method of breaking these emulsions at a specific desired stage. We report that long-chain alkyl amidine compounds can be reversibly transformed into charged surfactants by exposure to an atmosphere of carbon dioxide, thereby stabilizing water/alkane emulsions or, for the purpose of microsuspension polymerization, styrene-in-water emulsions. Bubbling nitrogen, argon, or air through the amidinium bicarbonate solutions at 65°C reverses the reaction, releasing carbon dioxide and breaking the emulsion. We also find that the neutral amidines function as switchable demulsifiers of an aqueous crude oil emulsion, enhancing their practical potential.

Surfactants are designed to stabilize emulsions during certain stages in cleaning, manufacturing, oil recovery, and other processes. Temporary emulsions (emulsions that are desired only during one stage of a process) are of practical interest in many areas, including (i) emulsion and microsuspension polymerizations, because of the low viscosity and efficient heat transfer compared with bulk polymerization; (ii) cleaning and metal degreasing of equipment; (iii) viscous oil transportation through pipelines, because the emulsion is far less viscous than the oil itself (*1*, *2*); (iv) enhanced oil-recovery (EOR), because surfactants help labilize oil by lowering the oil/water interfacial tension (*3*, *4*); (v) separation of oil from oil sands (*5*); and (vi) even some cosmetic emulsions which are intended to separate upon use (*6*). In these applications, an emulsion is only useful during one stage of a process, after which the surfactant becomes a liability that hinders separation of the components. The problem of how to break surfactant-stabilized temporary emulsions has not been resolved satisfactorily in the literature.

Cleavable or switchable surfactants could be used to address this problem, but they still have several drawbacks. A cleavable surfactant can be irreversibly converted, typically by application of a chemical or photochemical trigger, into one or more molecules with greatly reduced surface activity. This ability is usually conferred on the surfactant by incorporating a cleavable functional group such as an ester between the hydrophilic headgroup and the hydrophobic tail (*7*). A switchable surfactant, by contrast, can undergo fully reversible interconversions between active and inactive forms. Emulsions stabilized by either type of surfactant can thus be broken by application of the appropriate trigger. Solid materials such as particles that are temporarily protected by surfactants during synthesis can be deprotected and purified. Switchable surfactants have the additional advantages that their activity can be delayed until needed, they can be recovered and reused afterward, and their removal from the product stream can be facilitated by switching the surfactant to the form least soluble in the relevant medium.

At the same time, the nature of the trigger can limit the practical viability of cleavable and switchable surfactants. Triggers based on the addition of acids, bases, oxidants, or reductants suffer from economic and environmental costs, as well as the potential for product contamination or modification by these reagents. Mild and inexpensive triggers are therefore preferable. Photochemical approaches are hindered by the opacity of many emulsions. Surfactants in which the head-group functionality or the polarity of the tail can be switched electrochemically have been reported (*8*–*14*), but they contain expensive ferrocenyl groups, highly toxic viologen groups, or groups sensitive to O_2.

Here, we report switchable surfactants that use benign gases (CO_2 and air) as the triggers to switch them "on" and "off". The chemistry behind the transformation was uncovered during our earlier studies of amidine reactivity: On exposure to 1 atmosphere of gaseous CO_2, amidines mixed with water (*15*) or an alcohol (*16*) react exothermically to form the bicarbonate or alkylcarbonate salts. The reaction can be reversed by bubbling N_2 or Ar through the neat liquid salt, or else through a solution if the salt is a solid. We reasoned that an amidine with a long alkyl chain should be a poor surfactant but would become an effective surfactant on conversion to the charged amidinium bicarbonate by exposure to water and CO_2. A further benefit of the amidine systems is that the product generated by switching off the surfactant has negligible surface activity and water solubity—a substantial environmental advantage.

To evaluate this hypothesis, two such amidines, **1a** and **1b**, were prepared and characterized. Their reaction with CO_2 and water to produce amidinium bicarbonate salts (**2a** and **2b**) was confirmed by bubbling CO_2 through wet ether or wet acetonitrile solutions of **1a,b** and collecting and characterizing the precipitate (Reaction 1). The bicarbonate salts can be reconverted to the amidines by bubbling argon through solutions of **2a,b** in tetrahydrofuran; the products were isolated and their structures confirmed by ^{1}H nuclear magnetic resonance (NMR) and infrared (IR) spectroscopy. Thermogravimetric analysis of solid **2a** (fig. S1) showed that the CO_2 and water are driven off between 50 and 63°C (*17*).

The reversibility and repeatability of the process were confirmed by monitoring the conductivity of a solution of **1a** in wet dimethyl sulfoxide (DMSO) while CO_2 and then argon were bubbled through the solution over three cycles (Fig. 1). The conductivity rose when CO_2 was bubbled through the

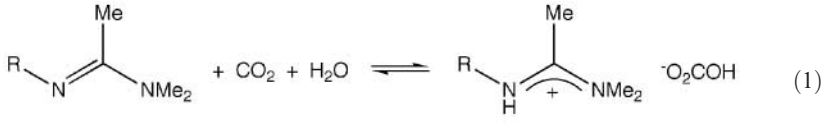

(1)

1a R = $C_{16}H_{33}$ **2a**
1b R = $C_{12}H_{25}$ **2b**

[1]Departments of Chemistry and Chemical Engineering, Queen's University, Kingston, Ontario K7L 3N6, Canada,. [2]Schools of Chemistry and Chemical Engineering, Georgia Institute of Technology, Atlanta, GA 30332–0100, USA.

*To whom correspondence should be addressed. E-mail: jessop@chem.queensu.ca

Two-Dimensional Nematic Colloidal Crystals Self-Assembled by Topological Defects

Igor Musevic, Miha Skarabot, Uros Tkalec, Miha Ravnik and Slobodan Zumer

Science **313** (5789), 954-958.
DOI: 10.1126/science.1129660